Propagation and Dephasing of Picosecond Phonon Polariton Pulses in Ammonium Chloride

G. M. Gale, F. Vallée, and C. Flytzanis
Laboratoire d'Optique Quantique du Centre National de la Recherche Scientifique, Ecole Polytechnique, 91128 Palaiseau Cedex, France
(Received 31 July 1986)

A space- and time-resolved coherent anti-Stokes Raman spectroscopy technique gives direct access to the propagation and loss of coherence of picosecond phonon-polariton pulses of widely varying wave vector and frequency in noncentrosymmetric crystals.

PACS numbers: 42.65.Dr, 42.65.Re, 78.30.Gt

The creation and measurement of ultrashort pulses of propagating collective excitation in crystals is a new and important problem in solid state physics, yielding novel information on crystal behavior via the temporal and spatial evolution of such pulses. In recent experiments,[1] femtosecond far-infrared pulses were generated and used to perform coherent time-domain spectroscopy of infrared and Raman-active modes in ferroelectrics. The selectivity of this technique is, however, limited, and the separation of temporal and spatial features is not straightforward.

We show in this Letter that it is possible to create and follow the spatial and temporal evolution in crystals of a picosecond pulse of propagating Raman-active polaritons by use of a time- and space-resolved coherent anti-Stokes Raman spectroscopy (CARS) technique. This method gives, for the first time, direct access to the energy propagation velocity and dephasing time of phonon polaritons over a large portion of the polariton dispersion curve, and imposes no restriction on polariton frequency. Furthermore, space- and time-resolved picosecond CARS allows direct study of the scattering of polaritons from spatial inhomogeneities (e.g., boundaries) and more generally opens up the field of polariton "acousto-optics."

We have performed the first demonstration of space- and time-resolved CARS on the phonon polariton associated with the ν_4 polar vibration in ammonium chloride, whose dispersion curves[2,3] and Raman spectra[4] have been extensively studied. The principle of the experiment is outlined in Fig. 1. Coherent excitation of the polariton at time $t=0$ and position $X=0$ is provided by two time-coincident optical picosecond pulses of wave vectors $\mathbf{k}_L$ and $\mathbf{k}_S$ and frequencies ω_L and ω_S, respectively. The polariton wave vector is $\mathbf{k}_\pi=\mathbf{k}_L-\mathbf{k}_S$, and, hence, its propagation direction is chosen by adjusting the angle between the two beams; and resonant excitation at $\omega_\pi(\mathbf{k}_\pi)$, the frequency of the polariton of wave vector $\mathbf{k}_\pi$, is obtained by frequency tuning ω_L such that $\omega_L-\omega_S=\omega_\pi$. Coupling with the light fields in the coherent excitation stage is described by a phenomenological energy density

$$V=(-d_E E_L E_S^* E_\pi^* - d_Q E_L E_S^* Q_\pi^*)+\text{c.c.}, \quad (1)$$

where E_L and E_S are the electric fields at ω_L (laser) and ω_S (Stokes), respectively, E_π and Q_π represent the electric field and transverse optical mechanical vibration associated with the polariton, and d_E and d_Q are coupling parameters which vary only slowly with polariton frequency.[5] This coupling produces a picosecond duration polariton wave packet at $t=0$ and $X=0$ which then propagates in the crystal in a direction determined by the polariton wave vector $\mathbf{k}_\pi=\mathbf{k}_L-\mathbf{k}_S$, and at a speed given by polariton group speed $V_g(\mathbf{k}_\pi)$. The temporal and spatial evolution of

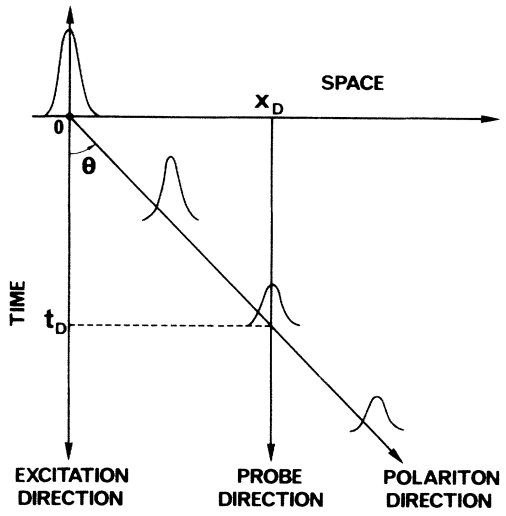

FIG. 1. Schematic outline of the experiment. The polariton wave packet, created by coherent scattering of picosecond laser and Stokes pulses, propagates in the crystal at an angle θ with respect to the excitation direction. This angle is determined by the excitation wave-vector geometry (see text). The coherent amplitude of the propagating wave packet may be measured by phase-matched coherent anti-Stokes scattering of a probe pulse suitably delayed in time (by t_D) and displaced in space (by X_D).

the propagating excitation is followed by phase-matched coherent anti-Stokes scattering at $\omega_a = \omega_p + \omega_\pi$ of a third pulse ω_p displaced with respect to the excitation in time (by t_D) and space (by X_D) (see Fig. 1). The measured dependence of the spatial displacement X_D, where the signal is maximum, on time delay t_D is directly related to the energy-propagation characteristics of the polariton wave packet.

The experimental system is driven by a mode-locked Nd^{3+}/glass laser system producing a single 5-ps pulse at 1.054 μm which is frequency converted to generate ω_p (18975 cm^{-1}), ω_S (16935 cm^{-1}), and ω_L (tunable 17900–18400 cm^{-1}). These three beams are focused into a 3- or 10-mm-long cooled NH_4Cl sample in a noncollinear k-matching geometry and the anti-Stokes signal is detected by a photomultiplier after suitable filtering. The results obtained for the polariton of frequency $\omega_\pi = 1300$ cm^{-1}, which has almost 50% photon and 50% phonon character,[6] are shown in Fig. 2, where we plot the measured position X_D of the peak coherent excitation as a function of probe delay t_D. The experimental points are well described by a straight line of slope P passing through the origin, and the polariton group velocity may thus be calculated from

$$V_g = P/(\sin\theta + P\eta\cos\theta/c),$$

where η is the crystal refractive index at the probe wavelength,[7] θ is the angle between the ω_L beam and the polariton propagation direction, and c is the speed of light in vacuum, yielding $V_g = (7.5 \pm 0.5) \times 10^9$ cm s^{-1} for the 1300-cm^{-1} polariton.

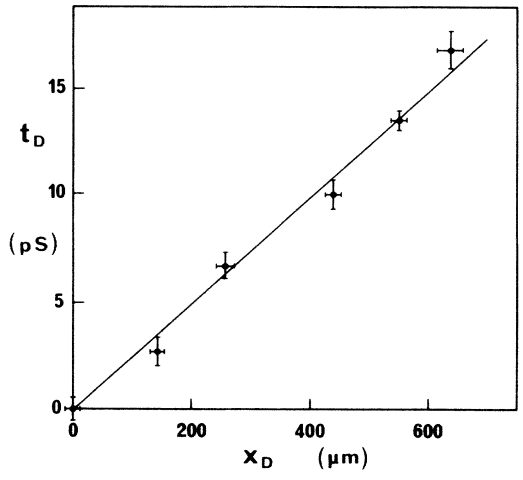

FIG. 2. The measured probe delay at which the coherent anti-Stokes signal scattered from the propagating polariton is maxium, as a function of lateral probe displacement from the excitation position. The slope of this line is directly related to polariton group velocity (see text).

The energy propagation velocity measured for various polariton frequencies is shown in Fig. 3. The observed energy propagation velocity varies strongly with polariton frequency from $\sim c/2$ at low frequency to $\sim c/50$ at high frequency. This large variation reflects the change in polariton character (from photonlike to phononlike) in the investigated frequency region. The polariton dispersion law in NH_4Cl has been extensively studied by Raman scattering[2,3] and the polariton wave vector may be reproduced (as the contribution from absorption is negligible in the frequency region of interest here) by the simple expression

$$k_\pi = 2\pi\tilde{\nu}_\pi \left(\epsilon_\infty \frac{\tilde{\nu}_{4l}^2 - \tilde{\nu}_\pi^2}{\tilde{\nu}_{4t}^2 - \tilde{\nu}_\pi^2} \right)^{1/2},$$

with $\tilde{\nu}_{4t} = 1400$ cm^{-1}, $\tilde{\nu}_{4l} = 1418$ cm^{-1}, and ϵ_∞ the optical dielectric constant. The group velocity may be calculated directly from the above expression by use of $V_g^{-1} = \partial k/\partial\omega$, and the full line in Fig. 3 shows the group velocity obtained in this manner. Agreement with the experimental points is excellent (there are no fitted parameters) and provides an indirect confirmation of our measurements of group velocity. Spatial or temporal spreading (due to velocity dispersion) of the polariton wave packet is small in our experiment and, hence, the intensity decrease of the peak ("followed polariton") coherent anti-Stokes signal with time delay and space displacement of the probe pulse gives directly the loss of coherence (T_2) of the polariton packet. Exponential time decay of polariton coherence is observed for all polaritons studied (between 1200 and 1380 cm^{-1}) except when the polariton interacts with the crystal exit surface. The results of these measurements at 78 K are shown in Fig. 4 where we plot the

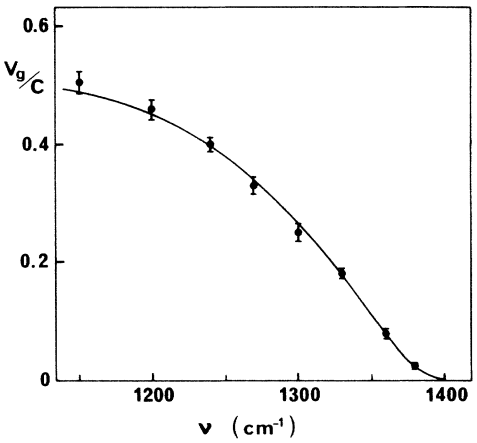

FIG. 3. Measured polariton group velocity V_g in NH_4Cl normalized to the speed of light in vacuum c (filled circles), as a function of polariton frequency. The full line is calculated with use of spectroscopic line positions (see text).

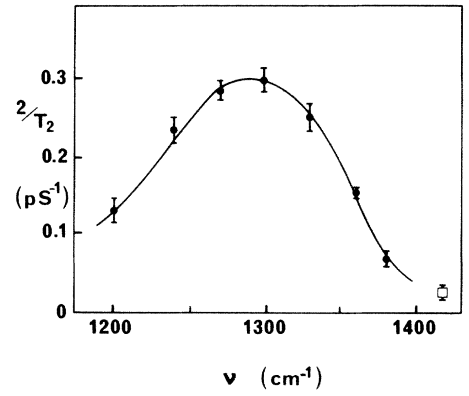

FIG. 4. Measured coherent decay rates $(2/T_2)$ for the ν_{4t} polariton in NH_4Cl as a function of polariton frequency in cm^{-1} (filled circles) at a crystal temperature of 78 K. Also shown (open square) is the decay rate at 78 K of the nonpropagating longitudinal component ν_{4l} at 1418 cm^{-1}.

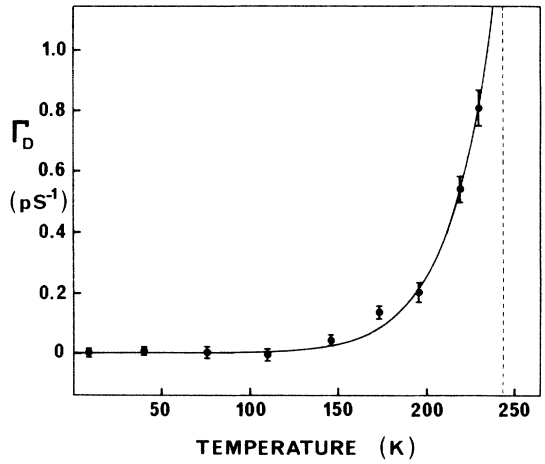

FIG. 5. Behavior of the strongly temperature-sensitive component Γ_D of the coherent relaxation rate of ν_{4t} at 1360 cm^{-1}. (The low-temperature residual rate Γ_π which is nearly temperature independent has been subtracterd.) Γ_D, defined to be zero at low temperature, increases rapidly as the order/disorder phase transition at 243 K (dotted line) is approached. The full line is a fit using $\Gamma_D = \gamma_D(1-L^2)$ where L is the order parameter of the crystal obtained from specific-heat data. Experimentally, Γ_D is essentially independent of polariton frequency.

observed decay rate $2/T_2$ as a function of polariton frequency ($\tilde{\nu}$ cm^{-1}). Also shown in Fig. 4 is the decay rate (open square) of the longitudinal (nonpropagating) component of ν_4 at 1418 cm^{-1}. A marked broad resonance-type dependence of decay rate on polariton frequency is observed at this temperature (78 K). The form of this dependence remains essentially unchanged as crystal temperature is lowered and decay rates decrease only slightly, by about 10%, at 7 K. However, as crystal temperature is increased above about 130 K a dramatic increase of relaxation rate occurs for all polaritons and relaxation times become subpicosecond as the order-disorder phase transition of this crystal at 243 K is approached.

The polariton is an admixture of an electromagnetic (photon) and a material (phonon) part and its damping Γ is certainly related to the way these two components are affected by the different lattice interactions and imperfections. Because this admixture arises through a coherent interaction of an electromagnetic mode and a material mode, there is no clear-cut way to locate the damping in any of these two components in particular.

In an ordered crystal the damping of polaritons is mainly due to the finite lifetime of their mechanical component Q_π in (1), which is anharmonically coupled to many phonon bands. This mechanism is the only one that has been considered[8] in the literature. It is particularly important in low-temperature ammonium chloride and can explain the frequency variation of the polariton damping rate (Fig. 4) which (with the phonon strength factor taken into account[6]) reflects the many-phonon density of states. This process gives only a weak temperature dependence of relaxation rate Γ_π, via Bose-Einstein occupation numbers, as experimentally observed between 7 and 130 K.

At higher temperature, in addition to the anharmonicity, the effects of disorder in the crystal become important and introduce an additional damping mechanism Γ_D which can directly affect the electromagnetic as well as the mechanical part of the polariton. The effect of disorder can be globally introduced with the order parameter L, deduced from specific heat data,[9] which begins to show significant deviation from its low-temperature value of $L=1$ at about 130 K, decreasing to $L=0$ at the phase-transition temperature of 243 K. If we set

$$\Gamma = \Gamma_\pi + \Gamma_D$$

for the total damping and subtract the essentially temperature-insensitive part Γ_π, a strong correlation is observed (see Fig. 5) between the high-temperature relaxation rate Γ_D and $(1-L^2)$, indicating that disorder makes an important contribution to coherence loss near the crystal phase transition.

In conclusion, we have shown that the space and time evolution of a propagating picosecond Raman-active phonon-polariton pulse in NH_4Cl may be directly followed by use of a space- and time-resolved CARS technique. This method should be immediately applicable in many other noncentrosymmetric crystals to the study of propagation and relaxation of phonon polaritons. This technique has also allowed us to study the scattering of the polariton from the crystal surface[10] and should give access to other important prob-

lems such as the interaction between polariton beams in crystals.

[1]D. H. Auston and K. P. Cheung, J. Opt. Soc. Am. B **2**, 606 (1985).

[2]V. S. Gorelik, O. P. Maximov, G. G. Mitin, and M. M. Sushchinskii, Solid State Commun. **21**, 615 (1977).

[3]G. G. Mitin, F. S. Gorekik, L. A. Kulevskii, Yu. N. Polivanov, and M. M. Sushchinskii, Zh. Eksp. Teor. Fiz. **69**, 450 (1976) [Sov. Phys. JETP **41**, 882 (1976)].

[4]C. H. Wang and R. B. Wright, J. Chem. Phys. **58**, 1411 (1973), and references therein.

[5]C. H. Henry and C. G. B. Garrett, Phys. Rev. **171**, 1058 (1968).

[6]R. Loudon, J. Phys. A **3**, 233 (1970).

[7]G. Poinsot and J. P. Mathieu, Ann. Phys. (Paris) **10**, 481 (1955).

[8]S. Ushioda, J. D. McMullen, and J. J. Delaney, Phys. Rev. B **8**, 4634 (1973).

[9]N. G. Parsonage and L. A. S. Staveley, in *Disorder in Crystals,* edited by N. G. Parsonage and L. A. Staveley (Clarendon, Oxford, 1978).

[10]G. M. Gale, F. Vallée, and C. Flytzanis, in "Dynamics of Molecular Crystals I" (Editions de Physique, Paris, to be published).